

# A network model of the modulation of gamma oscillations by NMDA receptors in cerebral cortex

<https://doi.org/10.1523/ENEURO.0157-23.2023>

**Cite as:** eNeuro 2023; 10.1523/ENEURO.0157-23.2023

Received: 13 May 2023

Revised: 31 August 2023

Accepted: 5 September 2023

---

*This Early Release article has been peer-reviewed and accepted, but has not been through the composition and copyediting processes. The final version may differ slightly in style or formatting and will contain links to any extended data.*

**Alerts:** Sign up at [www.eneuro.org/alerts](http://www.eneuro.org/alerts) to receive customized email alerts when the fully formatted version of this article is published.

Copyright © 2023 Susin and Destexhe

This is an open-access article distributed under the terms of the Creative Commons Attribution 4.0 International license, which permits unrestricted use, distribution and reproduction in any medium provided that the original work is properly attributed.

# A network model of the modulation of gamma oscillations by NMDA receptors in cerebral cortex

Eduarda Susin<sup>1,\*</sup>, Alain Destexhe<sup>1,†</sup>

<sup>1</sup>: Paris-Saclay University, Centre National de la Recherche Scientifique (CNRS),  
Institute of Neuroscience (NeuroPSI), Saclay, France

\* eduardadsusin@gmail.com, † alain.destexhe@cnrs.fr

September 6, 2023

**Abstract**—Psychotic drugs such as ketamine induce symptoms close to schizophrenia, and stimulate the production of gamma oscillations, as also seen in patients, but the underlying mechanisms are still unclear. Here, we have used computational models of cortical networks generating gamma oscillations, and have integrated the action of drugs such as ketamine to partially block n-methyl-d-Aspartate (NMDA) receptors. The model can reproduce the paradoxical increase of gamma oscillations by NMDA-receptor antagonists, assuming that antagonists affect NMDA receptors with higher affinity on inhibitory interneurons. We next used the model to compare the responsiveness of the network to external stimuli, and found that when NMDA channels are blocked, an increase of gamma power is observed altogether with an increase of network responsiveness. However, this responsiveness increase applies not only to gamma states, but also to asynchronous states with no apparent gamma. We conclude that NMDA antagonists induce an increased excitability state, which may or may not produce gamma oscillations, but the response to external inputs is exacerbated, which may explain phenomena such as altered perception or hallucinations.

**Index Terms**—Schizophrenia, NMDAR hypofunction, Gamma oscillations, Network Model, Psychosis

## Significance Statement

n-methyl-d-Aspartate (NMDA) synaptic receptors mediate excitatory interactions using the neurotransmitter glutamate. NMDA receptors have been implicated in psychosis such as schizophrenia and are also targeted by hallucinogenic drugs like Ketamine. However, the exact mechanisms of action are still unclear. Furthermore, Ketamine paradoxically leads to an excited state, while it is a blocker of NMDA receptors, therefore in principle diminishing excitation. Here, we use models of cortical networks generating gamma oscillations, and show that this model can explain the paradoxical exciting effect of Ketamine if one assumes a higher affinity on NMDA receptors of inhibitory interneurons. The simulated Ketamine effect reproduces known symptoms of psychosis such as increased gamma oscillations and exacerbated responses to external inputs, compatible with hallucinations.

## INTRODUCTION

SCHIZOPHRENIA is a mental disorder characterized by three classes of symptoms: positive symptoms (such as delusions, hallucinations and disordered thoughts or speech), negative symptoms (comprehending poverty of speech and

deficits of normal emotional response), and cognitive deficits (Lewis et al., 2005; Bozikas and Andreou, 2011; Su et al., 2018). Several abnormalities have been identified in schizophrenic patients, including important differences in neurotransmitters systems, anatomical deficits and abnormal neural rhythms (Uhlhaas and Singer, 2010; Shenton et al., 2001).

Gamma oscillations (30-90 Hz) in early-course schizophrenia patients are commonly reported to present increased power and/or phase synchronization (Flynn et al., 2008; Grent et al., 2018; Perrotelli et al., 2021). In parallel, positive correlation between psychotic symptoms and the gamma power have been identified in schizophrenic patients, in which higher gamma-band activity corresponded to increased symptom load (Mulert et al., 2011; Spencer et al., 2008, 2004, 2009). These findings indicate that hallucinations and delusions could be related to an excess of oscillatory synchronization in the gamma band.

NMDA receptor (NMDAR) antagonists, commonly used in sub-anesthetic doses as animal and human models to study Schizophrenia (Gunduz-Bruce, 2009), induce a psychotic state that resembles all three classes of symptoms of the disease (Javitt and Zukin, 1991; Krystal et al., 1994; Kalsi et al., 2011). Furthermore, NMDAR antagonists also increase gamma power amplitude, both in human and in animal models (Shaw et al., 2015; Plourde et al., 1997; Hong et al., 2010; Pinault, 2008; Kocsis, 2012; Wood et al., 2012; Nicolás et al., 2011; Slovák et al., 2017).

In this study we investigate by means of computational models how NMDAR antagonists, such as ketamine, affect the dynamics of neural networks and how the generated boosting of gamma activity affects the network response, providing an interpretation for the observed correlation between gamma power and psychotic episodes.

## MATERIALS AND METHODS

We describe the model used and the analysis procedures applied to the model.

### Neuronal Model

The model consists of a sparsely randomly connected network of excitatory and inhibitory spiking neurons, where the neural units are described by the *Adaptive Exponential*

*Integrate-And-Fire Model* (Adex) (Brette and Gerstner, 2005). In this model, each neuron  $i$  is described by its membrane potential  $V_i$ , which evolves according to the following equations:

$$C \frac{dV_i(t)}{dt} = -g_L(V_i - E_L) + g_L \Delta \exp \left[ \frac{(V_i(t) - V_{th})}{\Delta} \right] - w_i(t) - I_i^{Syn}(t)$$

$$\tau_{w_i} \frac{dw_i(t)}{dt} = a(V_i(t) - E_L) - w_i(t) + b \sum_j \delta(t - t_j) \quad (1)$$

where  $C$  is the membrane capacitance,  $g_L$  is the leakage conductance,  $E_L$  is the leaky membrane potential,  $V_{th}$  is the effective threshold,  $\Delta$  is the threshold slope factor and  $I_i^{Syn}(t)$  is postsynaptic current received by the neuron  $i$  (see next section). The adaptation current, described by the variable  $w_i$ , increases by an amount  $b$  every time the neuron  $i$  emits a spike at times  $t_j$  and decays exponentially with time scale  $\tau_w$ . The subthreshold adaptation is governed by the parameter  $a$ .

During the simulations, the equation characterizing the membrane potential  $V_i$  is numerically integrated until a spike is generated. Formally this happens when  $V_i$  grows rapidly toward infinity. In practice, the spiking time is defined as the moment in which  $V_i$  reaches a certain threshold ( $V_{th}$ ). When  $V_i = V_{th}$  the membrane potential is reset to  $V_{rest}$ , which is kept constant until the end of the refractory period  $T_{ref}$ . After the refractory period the equations start being integrated again.

In the developed network two types of cells were used: Regular Spiking (RS) excitatory cells and Fast Spiking (FS) inhibitory cells. The cell specific parameters are indicated in Table I.

TABLE I  
Specific Neuron Model Parameters

Parameter	RS	FS
$V_{th}$	-40 mV	-47.5 mV
$\Delta$	2 mV	0.5 mV
$T_{ref}$	5 ms	5 ms
$\tau_w$	500 ms	500 ms
$a$	4 nS	0 nS
$b$	20 pA	0 pA
$C$	150 pF	150 pF
$g_L$	10 nS	10 nS
$E_L$	-65 mV	-65 mV
$E_E$	0 mV	0 mV
$E_I$	-80 mV	-80 mV
$V_{rest}$	-65 mV	-65 mV

### Synaptic Models

The post-synaptic current received by each neuron  $i$  is composed by three components: two excitatory, referred to as  $AMPA$  and  $NMDA$  synaptic channels, and one inhibitory, referred to as  $GABA_A$  channels.

$$I_i^{Syn}(t) = I_i^{AMPA}(t) + I_i^{GABA_A}(t) + I_i^{NMDA}(t)$$

in which

$$I_i^{AMPA}(t) = G_i^{AMPA}(t)(V_i(t) - E^{AMPA})$$

$$I_i^{GABA_A}(t) = G_i^{GABA_A}(t)(V_i(t) - E^{GABA_A}) \quad (2)$$

$$I_i^{NMDA}(t) = G_i^{NMDA}(t)(V_i(t) - E^{NMDA})B(V_i(t))$$

$E^{AMPA} = 0$  mV,  $E^{GABA_A} = -80$  mV and  $E^{NMDA} = 0$  mV are the reversal potentials of  $AMPA$ ,  $GABA_A$  and  $NMDA$  channels. While the  $AMPA$  and  $GABA_A$ -mediated currents are fast,  $NMDA$  mediated currents are slower and voltage-dependent (Faber and Korn, 1980; Perouansky and Yaari, 1993; Götz et al., 1997; Bellingham et al., 1998). This voltage dependence, due to magnesium block, is accurately modeled by the phenomenological expression  $B(V)$  (Jahr and Stevens, 1990) :

$$B(V) = \frac{1}{1 + \exp(-0.062V) \cdot ([Mg^{2+}]_o / 3.57)} \quad (3)$$

where  $[Mg^{2+}]_o = 1$  mM is the external magnesium concentration (1 to 2 mM in physiological conditions).

Because of the fast dynamics of  $AMPA$  and  $GABA_A$  channels, their synaptic conductances ( $G^X$  with  $X=AMPA$ ,  $GABA_A$ ) are usually modeled to increase discontinuously by a discrete amount  $Q^X$ , every time a presynaptic neuron spikes at time  $t_k$ , and to subsequently decay exponentially with a decay time constant  $\tau_{decay}^X$  according to the following equation:

$$\tau_{decay}^X \frac{dG_i^X(t)}{dt} = -G_i^X(t) + Q^X \sum_k \delta(t - t_k) \quad (4)$$

In which,  $\sum_k$  runs over all the presynaptic spike times. The synaptic time constants used for  $AMPA$  and  $GABA_A$  synapses are  $\tau_{decay}^{AMPA} = 1.5$  ms and  $\tau_{decay}^{GABA_A} = 7.5$  ms.

$NMDA$  channels synaptic conductances,  $G^{NMDA}$ , because of their slow dynamics, are usually modeled as a bi-exponential function characterized by a rise time constant,  $\tau_{rise}^{NMDA} = 2$  ms, and a decay time constant  $\tau_{decay}^{NMDA} = 200$  ms, according to the following equation:

$$G_i^{NMDA} = Q_i^{NMDA} s_i(t)^{NMDA}$$

$$\frac{ds_i(t)^{NMDA}}{dt} = -\frac{s_i(t)^{NMDA}}{\tau_{decay}^{NMDA}} + \alpha x_i(t)(1 - s_i(t)^{NMDA})$$

$$\frac{dx_i(t)}{dt} = -\frac{x_i(t)}{\tau_{rise}^{NMDA}} + \sum_k \delta(t - t_k) \quad (5)$$

In which,  $Q_i^{NMDA}$  is the synaptic strength of the NMDA synapse towards the neuron  $i$ ,  $\alpha = 0.5/\text{ms}$  and  $x(t)$  is an auxiliary variable. The  $\sum_k$  runs over all the presynaptic spike times. Both,  $s(t)^{NMDA}$  and  $x(t)$ , are adimensional.

Synaptic strengths of *NMDA* synapses (towards RS and FS neurons) were chosen according to the parameter search expressed in Figure 1 ( $Q_R^{NMDA} = 0.4$  nS and  $Q_F^{NMDA} = 0.5$  nS), while the synaptic parameters of *AMPA* and *GABA<sub>A</sub>* synapses were chosen according to previous works Zerlaut and Destexhe (2017); Susin and Destexhe (2021) ( $Q^{AMPA} = 5$  nS and  $Q^{GABA_A} = 3.34$  nS). All synapses (*AMPA*, *GABA<sub>A</sub>* and *NMDA*) were delayed by time of 1.5 ms. With these choice of parameters the NMDA/AMPA charge ratio in the network is on average higher in RS cells then in FS cells (see Figure 2), in agreement with experimental measurements in prefrontal cortex of adult mice Rotaru et al. (2011) and rat Wang and Gao (2009).

#### Network Structure

The network developed in this work is composed of 5000 neurons (4000 RS and 1000 FS). Each neuron (RS or FS) was connected randomly to every other neurons in the network with a probability of 10%, receiving on average 500 excitatory synapses (mediated by both *AMPA* and *NMDA* channels) and 100 inhibitory synapses (mediated by *GABA<sub>A</sub>* channels).

#### External Input

In addition to recurrent connections, each neuron received an external drive to keep the network active. This external drive consisted of  $N_{ext} = 5000$  independent and identically distributed excitatory Poissonian spike trains with a spiking frequency  $\mu_{ext}$ . These spike trains were sent to the network with a 10% probability of connection and were computed inside of the synaptic current term  $I^{AMPA}$ , with a synaptic strength of  $Q_{Ext}^{AMPA} = 0.8$  nS. For gamma activity, the network was stimulated with a drive with  $\mu_{ext} = 3$  Hz. For Asynchronous and Irregular activity, the network was stimulated with a drive with  $\mu_{ext} = 2$  Hz. The external drive mimicked cortical input, like if the network was embedded in a much bigger one.

To inspected how the network responded to slowly-varying inputs (occurring in a time window much bigger than the Gamma period), an additional external input was included

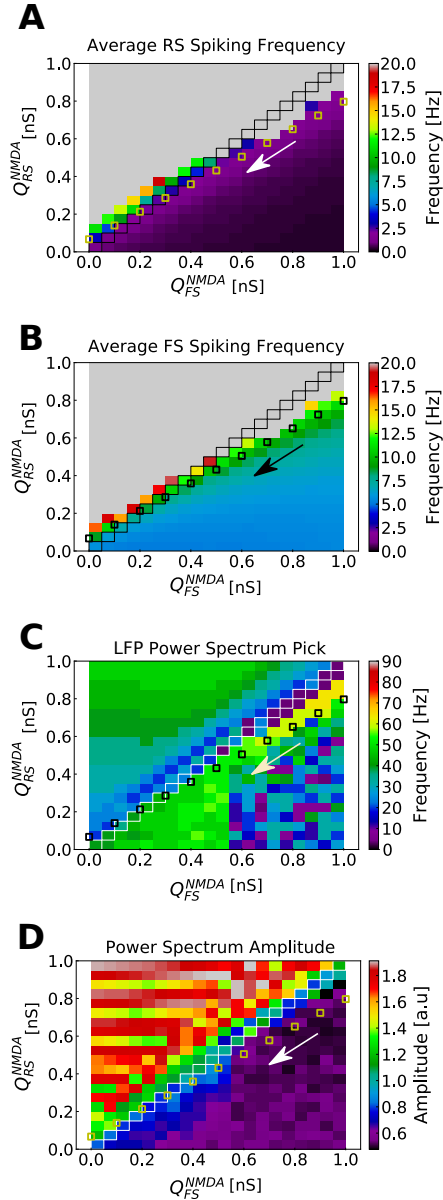


Fig. 1. **Parameter space of NMDA synaptic weights in RS and FS cells.** A) Average spiking rate in RS cells. B) Average spiking rate in FS cells. C) Population activity Power Spectrum pick. D) Population activity Power Spectrum amplitude. The parameter space of weights in NMDA synapses ( $Q^{NMDA}$ ) was explored for RS and FS cells in the developed network model.  $Q_{RS}^{NMDA}$  and  $Q_{FS}^{NMDA}$  varied from 0 nS to 1 nS in steps of 0.05 nS. Each point in the color maps corresponds to the average of 10 simulations of 5 seconds. Points in which  $Q_{RS}^{NMDA} = Q_{FS}^{NMDA}$  are highlighted. Small squares indicate a possible trajectory in the parameter space (in the direction of the arrow) generated by the action of NMDAR antagonists.

in the simulations. A simple way of generation this type of slowly varying stimulus is by means of a Gaussian variation in time of its amplitude. We have chosen Gaussian time variations with standard deviation of 50 ms to allow the stimulus to interact with at least three 60 Hz Gamma cycles. Several amplitudes were tested. This additional external input, similar to the external drive, also consisted of  $N_{ext} = 5000$  independent and identically distributed excitatory Poissonian spike trains, connected to the network with a 10% probability. The difference of this additional input was its firing rate time dependence ( $\mu_{ext}(t)$ ). These spike trains were computed inside of both synaptic current terms  $I^{AMPA}$  and  $I^{NMDA}$ , with a synaptic strengths of  $Q_{Ext}^{AMPA} = 0.8$  nS, and  $Q_{Ext}^{NMDA}$  and  $Q_{Ext}^{FS}$  as indicated in each case.

#### Block of NMDA channels: effect of NMDAR antagonists

In this work, we mimic the effect of NMDAR antagonists by changing the value of the NMDA synaptic weights  $Q^{NMDA}$ . In Fig. 3A, a possible trajectory in the parameter space generated by the action of NMDAR antagonists is depicted. This is one of many possible trajectories in parameters space (not shown).

#### Simulations

All neural networks were constructed using Brian2 simulator (Stimberg et al., 2019). All equations were numerically integrated using Euler Methods and  $dt=0.1$  ms as integration time step. The codes for each one of the three developed networks are available at ModelDB platform.

#### Population activity: LFP model

To measure the global behavior of the neuronal population, we used a simulated Local Field Potential (LFP). This LFP was generated by the network, by means of a recent method developed by (Telenczuk et al., 2020). This approach calculates the LFP by convolving the spike trains of the network with a Kernel that have been previously estimated from unitary LFPs (the LFP generated by a single axon,  $uLFP$ ) measured experimentally. Since this method assumes a spatial neuronal displacement, to be able to apply it to our simulations, we randomly displaced part of the network (50 neurons) in 2-D grid, assuming that the electrode was displaced on its center and was measuring the LFP in the same layer as neuronal soma. The program code of the kernel method is available in ModelDB (<http://modeldb.yale.edu/266508>), using python 3 or the *hoc* language of NEURON.

#### Power Spectrum

The Power Spectrum (or Power Spectral Density, PSD) of the simulated LFP was calculated by means of the Welch's method, using a Hamming window of length 0.25 seconds and 125 overlapping points. We used the Python-based ecosystem Scipy function *signal.welch* to do our calculations.

#### Distinction between gamma and asynchronous states

Because gamma oscillations and asynchronous-irregular states are usually part of a continuum of network states (Susin and Destexhe, 2021), we used a criterion based on the PSD to distinguish between gamma and AI states. The criterion was that if the oscillatory behavior of the network was prominent, which usually corresponds to a dominant peak at the gamma frequency in the PSD, then the network state was considered as gamma oscillation. If the PSD peak in the gamma frequency was either absent or small compared to the other fluctuations of the PSD, we considered the corresponding network state as AI. It is important to note that for most AI states, although the raster did not reveal any prominent oscillatory component, there was a small peak in the gamma frequency range. In general, the amplitude of the oscillation increased with depolarization of the neurons, as described previously (Susin and Destexhe, 2021).

#### Synaptic Charge

The synaptic charge (AMPA or NMDA) of each neuron is defined as the area under the curve of the average synaptic current (shaded areas of Fig. 2A or B), which was calculated from the presynaptic input time until 10 ms after it.

#### Responsiveness

The level of *responsiveness* ( $R$ ) of a network, due to an stimulus ( $S$ ) in a time window of duration  $T$ , is defined as the difference between the total number of spikes generated by the whole network due to an stimulus ( $N_{spikes}^S$ ) and the total number of spikes generated in the absence of the stimulus ( $N_{spikes}$ ), normalized by the network size (total number of neurons  $N_n$ ) and the duration of the time window  $T$ .

$$R = \frac{N_{spikes}^S - N_{spikes}}{TN_n} \quad (6)$$

## RESULTS

We first show that the computational model reproduces features of the block of NMDA receptors observed in cerebral cortex, and next, we investigate the responsiveness of the model in response to external input, comparing gamma oscillations with asynchronous states, which will constitute the main prediction of the model.

#### Computational model reproduces experimental features

As detailed in Methods, we used a network model of excitatory RS, and inhibitory FS cells, displaying gamma oscillations. This model includes available experimental data on the NMDA/AMPA charge ratio. This ratio is on average higher in RS cells than in FS cells (see Fig. 2), in agreement with experimental measurements in prefrontal cortex of adult mice (Rotaru et al., 2011) and rat (Wang and Gao, 2009).

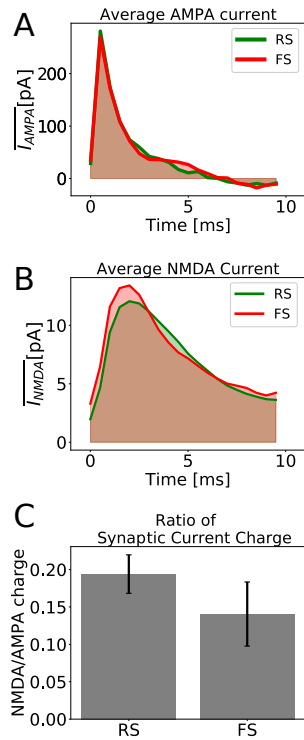


Fig. 2. **Excitatory synaptic currents.** A) Average AMPA current of one randomly picked RS (green) and one randomly picked FS (red) neuron. B) Average NMDA current of one randomly picked RS (green) and one randomly picked FS (red) neuron. C) Ratio of NMDA and AMPA charges for RS and FS cells. The synaptic charge ratio of each neuron was calculated separately. The Bars indicate the mean and the standard deviation among the RS and FS population. The NMDA synaptic strengths in RS and FS cells are  $Q_{RS}^{NMDA}=0.8$  nS and  $Q_{FS}^{NMDA}=1$  nS (which, in our model, describes a healthy condition).

Several preparations with sub-anesthetics doses of NMDAR antagonists have reported to produce neural excitation (Moghaddam et al., 1997; Lahti et al., 1995; Breier et al., 1997; Vollenweider et al., 1997; Suzuki et al., 2002; Jackson et al., 2004). Since NMDAR mediate excitatory synaptic transmission, this behavior is intriguing. Several hypothesis have been proposed to explain this apparent paradox (Su et al., 2018). One of the possible explanations is that NMDAR antagonists in sub-anesthetics doses act preferentially on inhibitory neurons, increasing network activity indirectly by means of disinhibition. Even though some contrasting results have been observed (Rotaru et al., 2011), this interpretation has been supported experimentally by several works (Homayoun and Moghaddam, 2007; Widman and McMahon, 2018; Zhang et al., 2008; Lazzaro et al., 2003). Network excitability have also been reported to increase in schizophrenic patients (Hoffman and Cavus, 2002; Daskalakis et al., 2007), and its increase in sensory and association cortex have been correlated with hallucinations (Hoffman et al., 2003; Merabet et al., 2003).

Another important effect of NMDAR antagonists in sub-

anesthetics doses is the increase of gamma-band activity. These observations were reported in human (Plourde et al., 1997; Hong et al., 2010; Shaw et al., 2015), monkey (Slovik et al., 2017) and rats (Pinault, 2008; Kocsis, 2012; Wood et al., 2012; Nicolás et al., 2011), both during cognitive tasks or free movement.

The network model developed in the present work (see Methods) is able to reproduce both of these features (increase of network excitability and increase of gamma power). Fig. 3 depicts the network behavior with respect to the to different NMDA synaptic strengths,  $Q^{NMDA}$ , in excitatory Regular Spiking (RS) and in inhibitory Fast Spiking (FS) cells. We mimic the block of NMDA channels due to the action of NMDAR antagonists by decreasing  $Q^{NMDA}$  in RS and FS cells according to Fig. 3A (see Methods). Points of higher synaptic strengths are associated with healthy conditions, while points with lower synaptic strengths are associated with pathological conditions supposedly similar to the schizophrenic brain. The properties of the synaptic input (average current and synaptic current charge), for different levels of NMDA block, are further shown in Fig. 4. The network dynamics for two sets of NMDA synaptic strengths are shown in Fig. 3B and Fig. 3C by means of a Raster Plot. As the synaptic strengths of NMDA channels decreased (higher concentration of NMDAR antagonists), the firing rate of excitatory RS cells increased while the firing rate of inhibitory FS cells decreased (Fig. 3D). In addition, the gamma power of the population activity (see Methods) presented an increase (Fig. 3E and F).

#### Network Responsiveness during gamma rhythms in different levels of NMDAR block

We investigated how the decrease of NMDA synaptic strength changed the network dynamics and its capacity to respond to external stimulus.

While network *excitability* relates to an overall increase of spiking activity, network *responsiveness* relates to the network capacity to react to a certain stimulus, producing additional spikes then the ones generated by spontaneous activity. These two dynamical measurements (excitability and responsiveness) are not always congruent, meaning that it is possible to observe an increase in excitability but a concomitant decrease in responsiveness (Susin and Destexhe, 2021).

Network responsiveness was defined as the difference between the total number of spikes generated by the whole network in the presence and in the absence of the stimulus (see Eq 6). We measured network responsiveness at different levels of NMDAR block for different stimulus amplitudes (Fig. 5). The stimulus consisted of a variation in time of the external Poissonian drive, in a Gaussian manner (see Methods).

Network responsiveness in RS cells increased with the increased level of NMDAR block, while the responsiveness of FS neurons decreased. In this case, both, network excitability and network responsiveness, behave in the same direction.

The increase of network responsiveness can be understood from Fig. 6. The NMDA receptors block depolarizes RS cells, while FS neurons are overall hyperpolarized. For weak levels of NMDA receptors block, no or weak depolarization is

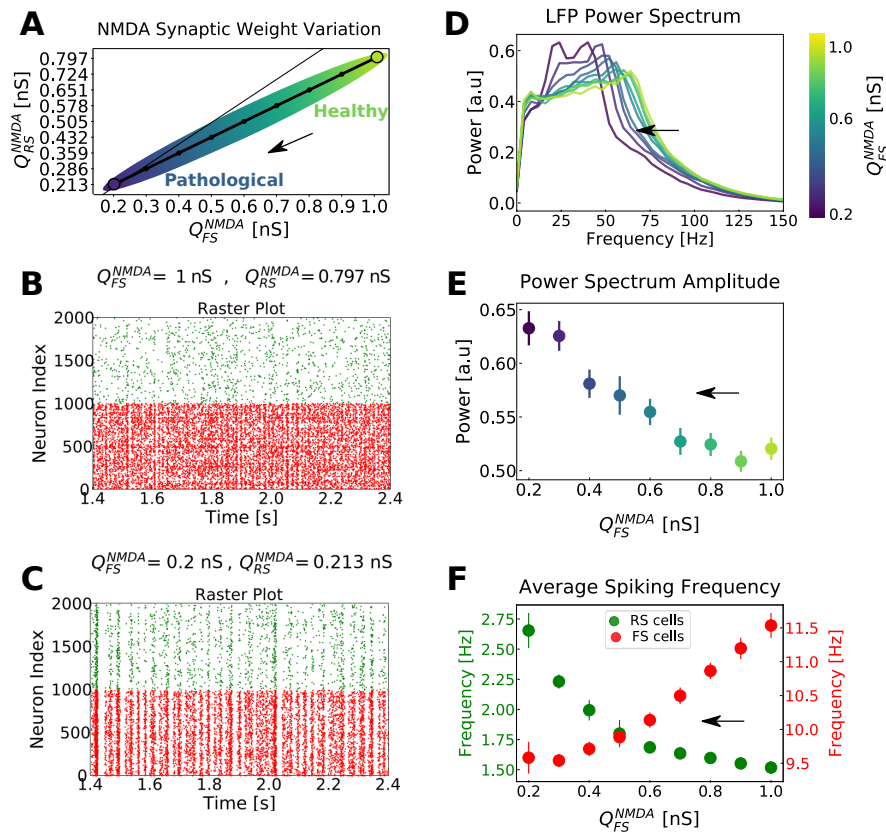


**Fig. 3. Network dynamics with respect to different levels of NMDA channels block in the network.** A) Possible trajectory in the parameter space of  $Q_{RS}^{NMDA}$  vs.  $Q_{FS}^{NMDA}$  (NMDA synaptic strengths in RS and FS cells), mimicking the action of NMDA receptor (NMDAR) antagonists (the higher the intensity of the NMDAR antagonists, the smaller the NMDA synaptic strengths; same trajectory as that indicated in Figure 1). The thin line indicates the identity for reference. The arrow indicates the progressive action of NMDAR antagonists. Points of higher synaptic strengths are associated with healthy conditions, while points with lower synaptic strengths are associated to pathological conditions supposedly similar to the schizophrenic brain. B) and C) Raster plots indicating the activity of only 1000 cells of each type (FS in red and RS in green), for two parameter sets. B:  $Q_{RS}^{NMDA} = 0.8$  nS and  $Q_{FS}^{NMDA} = 1$  nS, and C:  $Q_{RS}^{NMDA} = 0.213$  nS and  $Q_{FS}^{NMDA} = 0.2$  nS. D) Average normalized Power Spectrum of the network LFP for different NMDA synaptic strength. The synaptic strengths follow the curve indicated in A, but only the values in FS cells ( $Q_{FS}^{NMDA}$ ) are indicated in the color scale. Notice the shift of the Power Spectrum peak toward smaller frequencies with the increase of NMDA channel block. E) Power Spectrum peak amplitude with respect to the levels of NMDA channels block. Only the values of the NMDA synaptic strengths in FS cells ( $Q_{FS}^{NMDA}$ ) are indicated in the x axis. The color scheme (presented for better visualization) is the same as in D. Standard errors of the mean (SEM) are indicated as error bars. F) Average firing rate of RS (green) and FS cells (red) with respect to the trajectory in parameter space depicted in A. Like in E, only  $Q_{FS}^{NMDA}$  are indicated in the x axis. Standard errors of the mean (SEM) are indicated as error bars. Results expressed in D, E and F are the outcome of 50 simulations average. In all simulations, an external drive of 3Hz was used to maintain network activity in Gamma regime. See Methods.

observed in FS cells, while for strong levels of NMDA block a significant hyperpolarization is observed.

#### Gamma states vs. AI states

Gamma oscillations (30-90 Hz) are believed to be involved in information processing (Singer and Gray, 1995; Singer, 1999; O'Keefe and Recce, 1993; Fries et al., 2007; Fries, 2005, 2015), and have been associated to different high-level cognitive functions, such as memory (Pesaran et al., 2002; Colgin et al., 2009; Carr et al., 2012), perception (Rougeul-Buser et al., 1975; Bouyer et al., 1981; Rodriguez et al., 1999; Melloni et al., 2007), attention (Fries et al., 2001; Gregoriou

et al., 2009; Vinck et al., 2013; Rouhinen et al., 2013), focused arousal (Sheer, 1989) and prediction (Womelsdorf et al., 2006). In parallel, studies with schizophrenic patients have reported a positive correlation between psychotic symptoms and the power of gamma oscillations (Mulert et al., 2011; Spencer et al., 2008, 2004, 2009).

In contrast, Asynchronous-and-Irregular (AI) states (Brunel, 2000) are usually associated to conscious states (Koch et al., 2016), being observed during awake and aroused states (Goldman et al., 2019). This regime are characterized by irregular and sustained firing with very weak correlations (Softky and Koch, 1993; Holt et al., 1996; Shadlen and Newsome, 1998;

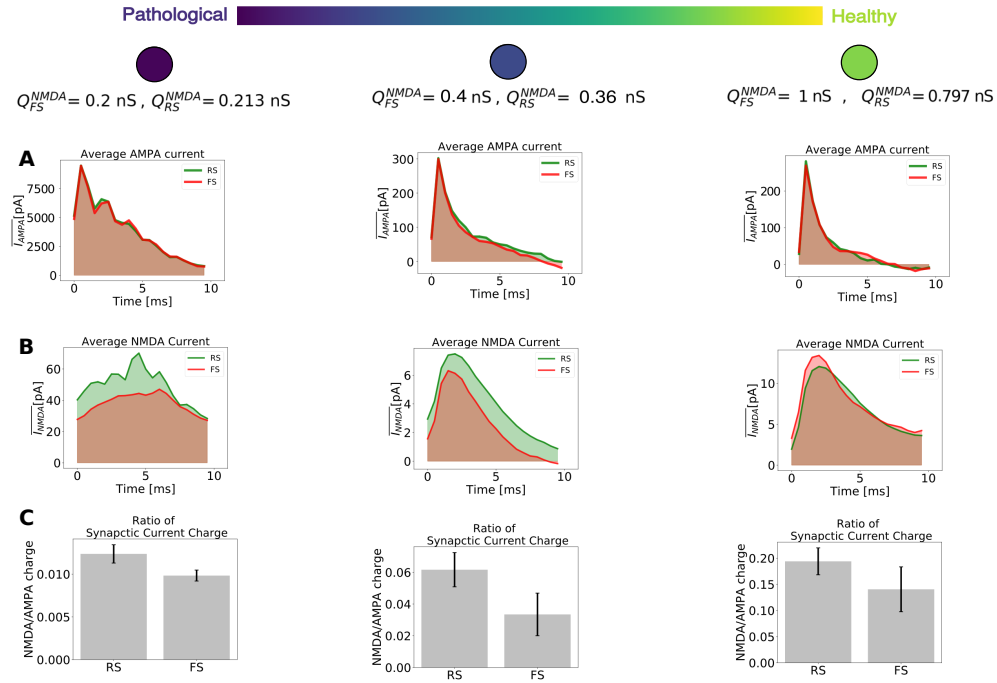


Fig. 4. **Excitatory synaptic currents with respect to different levels of NMDA channels block.** As in Figure 3, higher values of synaptic strengths are associated with healthy conditions, while lower values of synaptic strengths are associated to pathological conditions supposedly similar to the schizophrenic brain. A) Average AMPA current (for healthy and pathological conditions) of two randomly picked neurons : RS (green) and FS (red). B) Average NMDA current (for healthy and pathological conditions) of two randomly picked neurons : RS (green) and FS (red). C) Ratio of NMDA and AMPA charges for RS and FS cells (for healthy and pathological conditions). The synaptic charge ratio of each neuron was calculated separately. The Bars indicate the mean and the standard deviation among the RS and FS population.

Destexhe et al., 2003; Henrie and Shapley, 2005).

In a previous study (Susin and Destexhe, 2021) we reported that AI states, in comparison to oscillatory states in gamma band, provide the highest responsiveness to external stimuli, indicating that gamma oscillations tend to overall diminish responsiveness. This observation could indicate that gamma rhythms present a *masking effect*, conveying information in its cycles on spike timing at the expense of decreasing the strength of the network response.

In the present study, we compare AI and gamma states at different levels of NMDAR block. Fig. 7 depicts the responsiveness of RS neurons, with respect to different stimulus amplitudes (same protocol as Fig. 5), for different ensembles of NMDA synaptic strengths. In agreement with Fig. 5, parameter sets in which NMDA synaptic strengths are decreased (mimicking the action NMDAR antagonists) correspond to regions of the parameter space with higher responsiveness. For example,  $Q_{FS}^{NMDA} = 0.4$  nS and  $Q_{FS}^{NMDA} = 0.36$  nS displayed higher responsiveness than the networks in which the NMDA synaptic strengths were  $Q_{FS}^{NMDA} = 1$  nS and  $Q_{FS}^{NMDA} = 0.8$  nS. Interestingly, in both conditions, responsiveness in AI states were always superior to the one in gamma. This result was also observed in a similar model in the absence of NMDA channels (Susin and Destexhe, 2021). This example illustrates a general

tendency, which was also observed with other parameter sets. In particular, it was observed when NMDA currents had a faster decay time, as shown in the example of Fig. 8.

## DISCUSSION

In this work, we used computational models to investigate the effect of psychotic drugs such as ketamine in cerebral cortex, and how gamma oscillations relate to these effects. Our findings are (1) NMDA-receptor antagonists modulate the rhythms produced by a simple network model consisting of two distinct cell types, RS and FS cells, which generate gamma oscillations by means of the PING mechanism (Tiesinga and Sejnowski, 2009). This modulation is obtained assuming that the NMDAR block predominantly affects interneurons for low doses of ketamine. (2) The boosted gamma oscillations following partial block of NMDA receptors, was accompanied by an increased responsiveness to external inputs. (3) This increase of responsiveness could also be seen for asynchronous states, with no apparent gamma. We discuss below the implications of these findings.

A first prediction of the model is that it was necessary that the antagonism affects predominantly NMDAR receptors on interneurons. This feature is supported by a number of observations. Intuitively, if the NMDAR block would occur

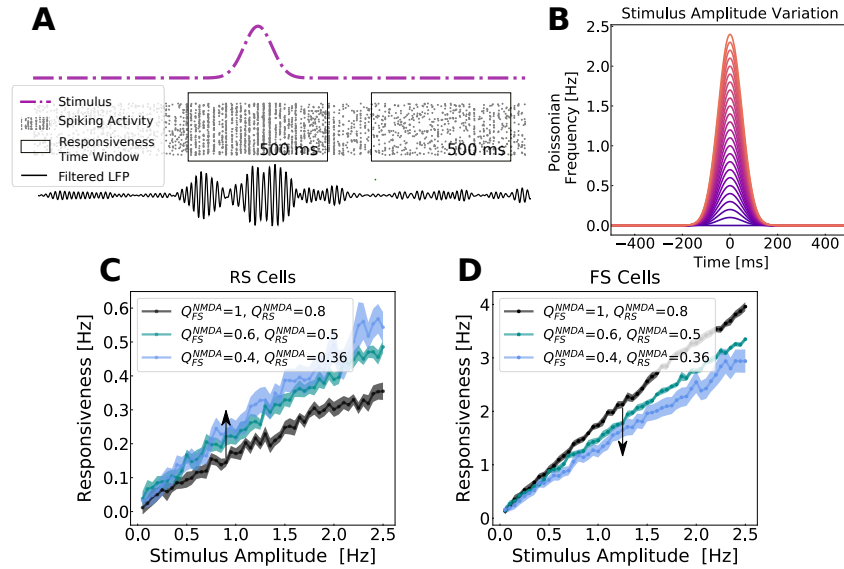


Fig. 5. **Network responsiveness to broad Gaussian inputs in different levels of NMDA channel blocked during gamma rhythms.** A) Responsiveness protocol scheme. The total number of spikes generated by the network were measured during an external stimulus and in its absence in a time window of 500 ms. The stimulus consisted of a Gaussian fluctuation in the firing rate of the external noise input. Responsiveness was calculated according to Equation 6. B) Gaussian input amplitude variation. The Gaussian amplitude varied from 0.05 Hz to 2.5 Hz (step of 0.05 Hz), always keeping the same standard deviation of 50 ms. C and D depict respectively the responsiveness of RS (C) and FS (D) neurons for different Gaussian amplitudes in different levels of NMDAR block, when the network was displaying gamma activity. The color-scheme indicates the synaptic weights of NMDA synapses ( $Q^{NMDA}$ ) in RS and FS cells. The arrow indicates the sense of the simulated action of NMDA antagonist (decreasing synaptic strength). Every point corresponds to the average responsiveness measured in 15 simulations. Standard error of the mean are indicated by the shaded region around each curve.

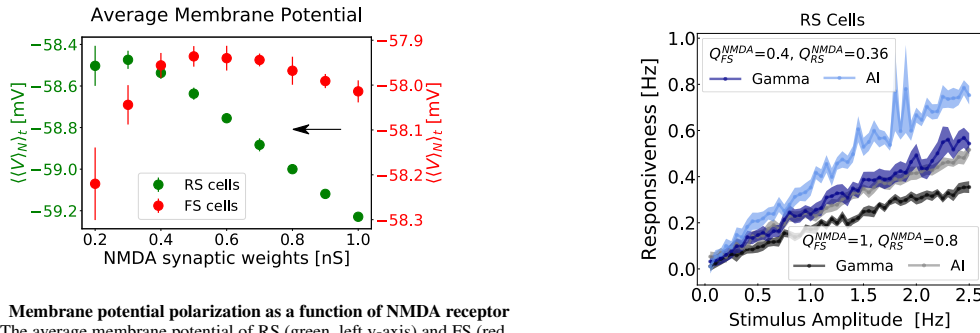


Fig. 6. **Membrane potential polarization as a function of NMDA receptor block.** The average membrane potential of RS (green, left y-axis) and FS (red, right y-axis) is expressed as function of NMDA synaptic weights of RS and FS cells. The values of  $Q_{RS}^{NMDA}$  and  $Q_{FS}^{NMDA}$  follow the same trajectory in the parameter space, as indicated in Fig. 3A. Only the values of  $Q_{FS}^{NMDA}$  are indicated in the x axis. The average was performed first in between neurons ( $\langle \rangle_N$ ), obtaining an average curve as a function of time, and subsequently with respect time ( $\langle \rangle_t$ ). The values plotted correspond to the average of  $\langle \langle V \rangle_N \rangle_t$  in between 10 simulations. The error bars indicate the standard error of the mean between these simulations.

Fig. 7. **Network responsiveness to broad Gaussian inputs of different amplitudes during gamma and AI states.** The responsiveness of RS neurons, due to different Gaussian amplitudes stimuli (same as in the protocol of Fig. 5), was measured in different states AI and gamma for NMDA synaptic parameter sets:  $Q_{RS}^{NMDA} = 0.8$  nS and  $Q_{FS}^{NMDA} = 1$  nS (Gamma: black, AI: gray), and  $Q_{RS}^{NMDA} = 0.36$  nS and  $Q_{FS}^{NMDA} = 0.4$  nS (Gamma: blue, AI: light blue). The Gaussian amplitude varied from 0.05 Hz to 2.5 Hz (step of 0.05 Hz), always keeping the same standard deviation of 50 ms.

predominantly on excitatory cells, then it is difficult to see how diminishing excitation could augment the activity and excitability of the network. This long-standing question was resolved recently by finding that indeed, NMDAR antagonists primarily affects NMDA receptors on interneurons. It was observed that the application of Ketamine or MK-801 in sub-anesthetic doses leads to an increased activity of glutamatergic

neurons both in cortex (Moghaddam et al., 1997; Lazzaro et al., 2003) and in hippocampus (Widman and McMahon, 2018), and that this increase of glutamatergic activity is a consequence of the disinhibition of GABAergic neurons (Homayoun and Moghaddam, 2007; Zhang et al., 2008). In addition, it has also been reported in hippocampus that

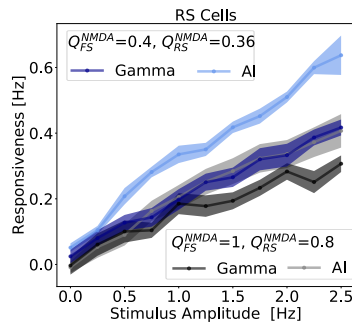


Fig. 8. **Network responsiveness with faster NMDA decay time constant.** As in Figure 7, the network responsiveness to broad Gaussian inputs of different amplitudes during gamma and AI states are displayed. In this case, the used NMDA synaptic times constant used in Equation 5 are  $\tau_{rise}^{NMDA} = 2$  ms and  $\tau_{decay}^{NMDA} = 50$  ms. The responsiveness of RS neurons, was measured in different states AI and gamma for NMDA synaptic parameter sets:  $Q_{FS}^{NMDA} = 0.8$  nS and  $Q_{RS}^{NMDA} = 1$  nS (Gamma: black, AI: gray), and  $Q_{FS}^{NMDA} = 0.36$  nS and  $Q_{RS}^{NMDA} = 0.4$  nS (Gamma: blue, AI: light blue). The Gaussian amplitude varied from 0.25 Hz to 2.5 Hz (step of 0.25 Hz), always keeping the same standard deviation of 50 ms. Every point corresponds to the average responsiveness measured in 10 simulations. Standard error of the mean are indicated by the shaded region around each curve..

inhibitory neurons are more sensitive to NMDAR antagonists than glutamatergic neurons (Ling and Benardo, 1995b; Grunze et al., 1996). Thus, our model completely supports these findings, and could reproduce the increase of gamma power induced by NMDA receptor antagonists. On the other hand, contrasting results also exist. For example, Rotaru et al. (2011) argue that NMDAR have less impact on the activity of inhibitory neurons than on the one of excitatory neurons, since they and other authors observed that NMDAR block depressed large EPSP-spike coupling more strongly in excitatory than in inhibitory neurons (Rotaru et al., 2011; Ling and Benardo, 1995a; Karayannis et al., 2007).

The second finding, which is probably the main finding of our study, is that the network has a marked increased responsiveness under the boosted gamma condition. This increased responsiveness could be tested experimentally either *in vitro*, by testing the response of cortical slices with and without application of NMDAR antagonists, or *in vivo*, by monitoring their response following administration of NMDA antagonists.

The third finding is that the increase of responsiveness is not specific to gamma oscillations, because it was also present for asynchronous states with no apparent gamma. The underlying mechanism is that the antagonism of NMDA receptors produce an overall depolarization of RS cells, and hyperpolarization of FS cells. Consequently, there is an increase of responsiveness of RS cells, with a corresponding decrease for FS cells, as we observed. In this model, the increase of responsiveness is due to the depolarizing effect on RS cells, and are not due to gamma oscillations. Indeed, the highest responsiveness was seen for asynchronous states, also in agreement with a previous modeling study (Susin and Destexhe, 2021).

### Possible implications to understand brain pathologies

Our model exhibits several interesting properties that can be related to pathologies. First, the model provides a possible explanation for the symptoms associated to ketamine and others NMDA receptor antagonists, such as hallucinations. The enhanced responsiveness produced by antagonizing NMDA receptors may explain exacerbated responses to sensory stimuli, which may be related to phenomena such as altered perception or hallucinations. Indeed, it is well documented that ketamine produces hallucinations together with a marked increase of gamma oscillations (Jones et al., 2012; Hakami et al., 2009; Lee et al., 2003).

Besides hallucinations, the model seems also a priori consistent with the previously reported role for FS neurons in schizophrenia. Post-mortem analysis of schizophrenic patient brains have shown a reduced expression of parvalbumin (PV) and GAD67 (Akbarian et al., 1995; Volk et al., 2000; Akbarian and Huang, 2006; Inan et al., 2013; Eyles et al., 2002; Lewis et al., 2005). In parallel, genetic ablation of NMDA receptors in PV-positive interneurons in rodents mimics important behavioral (Korotkova et al., 2010) and phenotypical features of the disease (reduction of GAD67 (Belforte et al., 2010), increase of neuronal excitability (Belforte et al., 2010) and increase of spontaneous gamma power (Carlen et al., 2012; Billingslea et al., 2014; Nakao and Nakazawa, 2014)). These observations support the idea that the hypofunction of NMDA receptors in PV-positive interneurons are specially important in this illness.

However, NMDA receptors are expressed in both GABAergic and glutamatergic neurons (Homayoun and Moghaddam, 2007), and it still remains unclear in which types of cells the NMDA receptor hypofunction causes schizophrenia (Gonzalez-Burgos and Lewis, 2012; Su et al., 2018). Some works reported conflicting results and have questioned the hypothesis that PV-positive Fast Spiking neurons play a role in Schizophrenia (Rotaru et al., 2011; Gonzalez-Burgos and Lewis, 2012).

In our model, the effect of NMDAR antagonists is to increase excitability due to disinhibition, consistent with a number of experimental observations (Moghaddam et al., 1997; Lahti et al., 1995; Breier et al., 1997; Vollenweider et al., 1997; Suzuki et al., 2002; Jackson et al., 2004). This increased excitability is accompanied by a gamma power increase, as also found in experiments with ketamine (Plourde et al., 1997; Hong et al., 2010; Shaw et al., 2015) or in schizophrenic patients (Flynn et al., 2008; Grent et al., 2018; Perrotelli et al., 2021; Mulert et al., 2011; Spencer et al., 2008, 2004, 2009). The model could reproduce all these experimental observations only assuming a larger decrease of the NMDA synaptic strengths in FS cells than in RS cells (see Fig. 3A). These results support the idea sustained by some authors (Gonzalez-Burgos and Lewis, 2008), that PV-positive Fast Spiking inhibitory neurons play a key role in schizophrenia. Another modeling study also stressed the importance of NMDA channels into FS neurons (Spencer, 2009). Thus, models support the view that the hypofunction of NMDA receptors on FS cells could explain a number of

features typical of schizophrenia, such as anomalous responses and boosted gamma oscillations.

#### ACKNOWLEDGMENTS AND FUNDING SOURCES

This research was supported by the Centre National de la Recherche Scientifique (CNRS) and the European Community (Human Brain Project, H2020-785907). E.S. acknowledges a PhD fellowship from the École des Neurosciences de Paris (ENP) and from the Fondation pour la Recherche Médicale (FRM) - grant FDT202012010566 and the financial support from La Fondation des Treilles.

#### REFERENCES

- Akbadian, S., Huang, H.S., 2006. Molecular and cellular mechanisms of altered *gad1/gad67* expression in schizophrenia and related disorders. *Brain research reviews* 52, 293–304.
- Akbadian, S., Kim, J.J., Potkin, S.G., Hagman, J.O., Tafazzoli, A., Bunney, W.E., Jones, E.G., 1995. Gene expression for glutamic acid decarboxylase is reduced without loss of neurons in prefrontal cortex of schizophrenics. *Archives of general psychiatry* 52, 258–266.
- Belforte, J.E., Zsiris, V., Sklar, E.R., Jiang, Z., Yu, G., Li, Y., Quinlan, E.M., Nakazawa, K., 2010. Postnatal *nmda* receptor ablation in corticolimbic interneurons confers schizophrenia-like phenotypes. *Nature neuroscience* 13, 76–83.
- Bellingham, M.C., Lim, R., Walmsley, B., 1998. Developmental changes in *epsc* quantal size and quantal content at a central glutamatergic synapse in rat. *The Journal of Physiology* 511, 861–869.
- Billingslea, E.N., Tatar-Leitman, V.M., Anguiano, J., Jutzeler, C.R., Suh, J., Saunders, J.A., Morita, S., Featherstone, R.E., Ortinski, P.I., Gandal, M.J., et al., 2014. Parvalbumin cell ablation of *nmda-r1* causes increased resting network excitability with associated social and self-care deficits. *Neuropsychopharmacology* 39, 1603–1613.
- Bouyer, J., Montaron, M., Rougeul, A., 1981. Fast frontoparietal rhythms during combined focused attentive behaviour and immobility in cat: cortical and thalamic localizations. *Electroencephalography and clinical neurophysiology* 51, 244–252.
- Bozikas, V.P., Andreou, C., 2011. Longitudinal studies of cognition in first episode psychosis: a systematic review of the literature. *Australian & New Zealand Journal of Psychiatry* 45, 93–108.
- Breier, A., Malhotra, A.K., Pinals, D.A., Weisenfeld, N.I., Pickar, D., 1997. Association of ketamine-induced psychosis with focal activation of the prefrontal cortex in healthy volunteers. *The American journal of psychiatry*.
- Brette, R., Gerstner, W., 2005. Adaptive exponential integrate-and-fire model as an effective description of neuronal activity. *Journal of neurophysiology* 94, 3637–3642.
- Brunel, N., 2000. Dynamics of sparsely connected networks of excitatory and inhibitory spiking neurons. *Journal of computational neuroscience* 8, 183–208.
- Carlen, M., Meletis, K., Siegle, J., Cardin, J., Futai, K., Vierling-Claassen, D., Ruehlmann, C., Jones, S.R., Deisseroth, K., Sheng, M., et al., 2012. A critical role for *nmda* receptors in parvalbumin interneurons for gamma rhythm induction and behavior. *Molecular psychiatry* 17, 537–548.
- Carr, M.F., Karlsson, M.P., Frank, L.M., 2012. Transient slow gamma synchrony underlies hippocampal memory replay. *Neuron* 75, 700–713.
- Colgin, L.L., Denninger, T., Fyhn, M., Hafting, T., Bonnevie, T., Jensen, O., Moser, M.B., Moser, E.I., 2009. Frequency of gamma oscillations routes flow of information in the hippocampus. *Nature* 462, 353–357.
- Daskalakis, Z.J., Fitzgerald, P.B., Christensen, B.K., 2007. The role of cortical inhibition in the pathophysiology and treatment of schizophrenia. *Brain research reviews* 56, 427–442.
- Destexhe, A., Rudolph, M., Paré, D., 2003. The high-conductance state of neocortical neurons in vivo. *Nature reviews neuroscience* 4, 739–751.
- Eyles, D., McGrath, J., Reynolds, G., 2002. Neuronal calcium-binding proteins and schizophrenia. *Schizophrenia research* 57, 27–34.
- Faber, D.S., Korn, H., 1980. Single-shot channel activation accounts for duration of inhibitory postsynaptic potentials in a central neuron. *Science* 208, 612–615.
- Flynn, G., Alexander, D., Harris, A., Whitford, T., Wong, W., Galletly, C., Silverstein, S., Gordon, E., Williams, L.M., 2008. Increased absolute magnitude of gamma synchrony in first-episode psychosis. *Schizophrenia research* 105, 262–271.
- Fries, P., 2005. A mechanism for cognitive dynamics: neuronal communication through neuronal coherence. *Trends in cognitive sciences* 9, 474–480.
- Fries, P., 2015. Rhythms for cognition: communication through coherence. *Neuron* 88, 220–235.
- Fries, P., Nikolić, D., Singer, W., 2007. The gamma cycle. *Trends in neurosciences* 30, 309–316.
- Fries, P., Reynolds, J.H., Rorie, A.E., Desimone, R., 2001. Modulation of oscillatory neuronal synchronization by selective visual attention. *Science* 291, 1560–1563.
- Goldman, J.S., Tort-Colet, N., Di Volo, M., Susin, E., Bouté, J., Dali, M., Carlu, M., Nghiem, T.A., Górski, T., Destexhe, A., 2019. Bridging single neuron dynamics to global brain states. *Frontiers in systems neuroscience* 13, 75.
- Gonzalez-Burgos, G., Lewis, D.A., 2008. Gaba neurons and the mechanisms of network oscillations: implications for understanding cortical dysfunction in schizophrenia. *Schizophrenia bulletin* 34, 944–961.
- Gonzalez-Burgos, G., Lewis, D.A., 2012. *Nmda* receptor hypofunction, parvalbumin-positive neurons, and cortical gamma oscillations in schizophrenia. *Schizophrenia bulletin* 38, 950–957.
- Götz, T., Kraushaar, U., Geiger, J., Lübke, J., Berger, T., Jonas, P., 1997. Functional properties of *ampa* and *nmda* receptors expressed in identified types of basal ganglia neurons. *Journal of Neuroscience* 17, 204–215.
- Gregoriou, G.G., Gotts, S.J., Zhou, H., Desimone, R., 2009. High-frequency, long-range coupling between prefrontal and visual cortex during attention. *science* 324, 1207–1210.
- Grent, T., Gross, J., Goense, J., Wibrall, M., Gajwani, R., Gumley, A.I., Lawrie, S.M., Schwannauer, M., Schultze-

- Lutter, F., Schröder, T.N., et al., 2018. Resting-state gamma-band power alterations in schizophrenia reveal *e/i*-balance abnormalities across illness-stages. *Elife* 7, e37799.
- Grunze, H.C., Rainnie, D.G., Hasselmo, M.E., Barkai, E., Hearn, E.F., McCarley, R.W., Greene, R.W., 1996. Nmda-dependent modulation of cal local circuit inhibition. *Journal of Neuroscience* 16, 2034–2043.
- Gunduz-Bruce, H., 2009. The acute effects of nmda antagonism: from the rodent to the human brain. *Brain research reviews* 60, 279–286.
- Hakami, T., Jones, N.C., Tolmacheva, E.A., Gaudias, J., Chaumont, J., Salzberg, M., O'Brien, T.J., Pinault, D., 2009. Nmda receptor hypofunction leads to generalized and persistent aberrant  $\gamma$  oscillations independent of hyperlocomotion and the state of consciousness. *PloS one* 4, e6755.
- Henrie, J.A., Shapley, R., 2005. Lfp power spectra in v1 cortex: the graded effect of stimulus contrast. *Journal of neurophysiology* 94, 479–490.
- Hoffman, R.E., Cavus, I., 2002. Slow transcranial magnetic stimulation, long-term depotentiation, and brain hyperexcitability disorders. *American Journal of Psychiatry* 159, 1093–1102.
- Hoffman, R.E., Hawkins, K.A., Gueorguieva, R., Boutros, N.N., Rachid, F., Carroll, K., Krystal, J.H., 2003. Transcranial magnetic stimulation of left temporoparietal cortex and medication-resistant auditory hallucinations. *Archives of general psychiatry* 60, 49–56.
- Holt, G.R., Softky, W.R., Koch, C., Douglas, R.J., 1996. Comparison of discharge variability in vitro and in vivo in cat visual cortex neurons. *Journal of neurophysiology* 75, 1806–1814.
- Homayoun, H., Moghaddam, B., 2007. Nmda receptor hypofunction produces opposite effects on prefrontal cortex interneurons and pyramidal neurons. *Journal of Neuroscience* 27, 11496–11500.
- Hong, L.E., Summerfelt, A., Buchanan, R.W., O'donnell, P., Thaker, G.K., Weiler, M.A., Lahti, A.C., 2010. Gamma and delta neural oscillations and association with clinical symptoms under subanesthetic ketamine. *Neuropsychopharmacology* 35, 632–640.
- Inan, M., Petros, T.J., Anderson, S.A., 2013. Losing your inhibition: linking cortical gabaergic interneurons to schizophrenia. *Neurobiology of disease* 53, 36–48.
- Jackson, M.E., Homayoun, H., Moghaddam, B., 2004. Nmda receptor hypofunction produces concomitant firing rate potentiation and burst activity reduction in the prefrontal cortex. *Proceedings of the National Academy of Sciences* 101, 8467–8472.
- Jahr, C.E., Stevens, C.F., 1990. Voltage dependence of nmda-activated macroscopic conductances predicted by single-channel kinetics. *Journal of Neuroscience* 10, 3178–3182.
- Javitt, D.C., Zukin, S.R., 1991. Recent advances in the phenylcyclidine model of schizophrenia. *The American journal of psychiatry*.
- Jones, N.C., Reddy, M., Anderson, P., Salzberg, M.R., O'Brien, T.J., Pinault, D., 2012. Acute administration of typical and atypical antipsychotics reduces eeg gamma power, but only the preclinical compound ly379268 reduces the ketamine-induced rise in gamma power. *International Journal of Neuropsychopharmacology* 15, 657–668.
- Kalsi, S.S., Wood, D.M., Dargan, P.I., 2011. The epidemiology and patterns of acute and chronic toxicity associated with recreational ketamine use. *Emerging Health Threats Journal* 4, 7107.
- Karayannis, T., Huerta-Ocampo, I., Capogna, M., 2007. Gabaergic and pyramidal neurons of deep cortical layers directly receive and differently integrate callosal input. *Cerebral Cortex* 17, 1213–1226.
- Koch, C., Massimini, M., Boly, M., Tononi, G., 2016. Neural correlates of consciousness: progress and problems. *Nature Reviews Neuroscience* 17, 307–321.
- Kocsis, B., 2012. Differential role of nr2a and nr2b subunits in n-methyl-d-aspartate receptor antagonist-induced aberrant cortical gamma oscillations. *Biological psychiatry* 71, 987–995.
- Korotkova, T., Fuchs, E.C., Ponomarenko, A., von Engelhardt, J., Monyer, H., 2010. Nmda receptor ablation on parvalbumin-positive interneurons impairs hippocampal synchrony, spatial representations, and working memory. *Neuron* 68, 557–569.
- Krystal, J.H., Karper, L.P., Seibyl, J.P., Freeman, G.K., Delaney, R., Bremner, J.D., Heninger, G.R., Bowers, M.B., Charney, D.S., 1994. Subanesthetic effects of the non-competitive nmda antagonist, ketamine, in humans: psychotomimetic, perceptual, cognitive, and neuroendocrine responses. *Archives of general psychiatry* 51, 199–214.
- Lahti, A.C., Holcomb, H.H., Medoff, D.R., Tamminga, C.A., 1995. Ketamine activates psychosis and alters limbic blood flow in schizophrenia. *Neuroreport* 6, 869–872.
- Lazzaro, V.D., Oliviero, A., Profice, P., Pennisi, M., Pilato, F., Zito, G., Dileone, M., Nicoletti, R., Pasqualetti, P., Tonali, P., 2003. Ketamine increases human motor cortex excitability to transcranial magnetic stimulation. *The Journal of physiology* 547, 485–496.
- Lee, K.H., Williams, L.M., Breakspear, M., Gordon, E., 2003. Synchronous gamma activity: a review and contribution to an integrative neuroscience model of schizophrenia. *Brain Research Reviews* 41, 57–78.
- Lewis, D.A., Hashimoto, T., Volk, D.W., 2005. Cortical inhibitory neurons and schizophrenia. *Nature Reviews Neuroscience* 6, 312–324.
- Ling, D., Benardo, L.S., 1995a. Recruitment of gabaa inhibition in rat neocortex is limited and not nmda dependent. *Journal of Neurophysiology* 74, 2329–2335.
- Ling, D.S., Benardo, L.S., 1995b. Activity-dependent depression of monosynaptic fast ipscs in hippocampus: contributions from reductions in chloride driving force and conductance. *Brain research* 670, 142–146.
- Melloni, L., Molina, C., Pena, M., Torres, D., Singer, W., Rodriguez, E., 2007. Synchronization of neural activity across cortical areas correlates with conscious perception. *Journal of neuroscience* 27, 2858–2865.
- Merabet, L.B., Kobayashi, M., Barton, J., Pascual-Leone, A., 2003. Suppression of complex visual hallucinatory experiences by occipital transcranial magnetic stimulation: a case report. *Neurocase* 9, 436–440.

- Moghaddam, B., Adams, B., Verma, A., Daly, D., 1997. Activation of glutamatergic neurotransmission by ketamine: a novel step in the pathway from nmda receptor blockade to dopaminergic and cognitive disruptions associated with the prefrontal cortex. *Journal of Neuroscience* 17, 2921–2927.
- Mulert, C., Kirsch, V., Pascual-Marqui, R., McCarley, R.W., Spencer, K.M., 2011. Long-range synchrony of gamma oscillations and auditory hallucination symptoms in schizophrenia. *International Journal of Psychophysiology* 79, 55–63.
- Nakao, K., Nakazawa, K., 2014. Brain state-dependent abnormal lfp activity in the auditory cortex of a schizophrenia mouse model. *Frontiers in neuroscience* 8, 168.
- Nicolás, M.J., López-Azcárate, J., Valencia, M., Alegre, M., Pérez-Alcázar, M., Iriarte, J., Artieda, J., 2011. Ketamine-induced oscillations in the motor circuit of the rat basal ganglia. *PloS one* 6, e21814.
- O'Keefe, J., Recce, M.L., 1993. Phase relationship between hippocampal place units and the eeg theta rhythm. *Hippocampus* 3, 317–330.
- Perouansky, M., Yaari, Y., 1993. Kinetic properties of nmda receptor-mediated synaptic currents in rat hippocampal pyramidal cells versus interneurons. *The Journal of Physiology* 465, 223–244.
- Perrottelli, A., Giordano, G.M., Brando, F., Giuliani, L., Mucci, A., 2021. Eeg-based measures in at-risk mental state and early stages of schizophrenia: A systematic review. *Frontiers in psychiatry* 12, 582.
- Pesaran, B., Pezaris, J.S., Sahani, M., Mitra, P.P., Andersen, R.A., 2002. Temporal structure in neuronal activity during working memory in macaque parietal cortex. *Nature neuroscience* 5, 805–811.
- Pinault, D., 2008. N-methyl d-aspartate receptor antagonists ketamine and mk-801 induce wake-related aberrant  $\gamma$  oscillations in the rat neocortex. *Biological psychiatry* 63, 730–735.
- Plourde, G., Baribeau, J., Bonhomme, V., 1997. Ketamine increases the amplitude of the 40-hz auditory steady-state response in humans. *British journal of anaesthesia* 78, 524–529.
- Rodriguez, E., George, N., Lachaux, J.P., Martinerie, J., Renault, B., Varela, F.J., 1999. Perception's shadow: long-distance synchronization of human brain activity. *Nature* 397, 430–433.
- Rotaru, D.C., Yoshino, H., Lewis, D.A., Ermentrout, G.B., Gonzalez-Burgos, G., 2011. Glutamate receptor subtypes mediating synaptic activation of prefrontal cortex neurons: relevance for schizophrenia. *Journal of Neuroscience* 31, 142–156.
- Rougeul-Buser, A., Bouyer, J., Buser, P., 1975. From attentiveness to sleep. a topographical analysis of localized "synchronized" activities on the cortex of normal cat and monkey. *Acta Neurobiol Exp (Warsz)* 35, 805–19.
- Rouhinen, S., Panula, J., Palva, J.M., Palva, S., 2013. Load dependence of  $\beta$  and  $\gamma$  oscillations predicts individual capacity of visual attention. *Journal of Neuroscience* 33, 19023–19033.
- Shadlen, M.N., Newsome, W.T., 1998. The variable discharge of cortical neurons: implications for connectivity, computation, and information coding. *Journal of neuroscience* 18, 3870–3896.
- Shaw, A.D., Saxena, N., Jackson, L.E., Hall, J.E., Singh, K.D., Muthukumaraswamy, S.D., 2015. Ketamine amplifies induced gamma frequency oscillations in the human cerebral cortex. *European Neuropsychopharmacology* 25, 1136–1146.
- Sheer, D.E., 1989. Focused arousal and the cognitive 40-hz event-related potentials: differential diagnosis of alzheimer's disease. *Progress in clinical and biological research* 317, 79–94.
- Shenton, M.E., Dickey, C.C., Frumin, M., McCarley, R.W., 2001. A review of mri findings in schizophrenia. *Schizophrenia research* 49, 1–52.
- Singer, W., 1999. Neuronal synchrony: a versatile code for the definition of relations? *Neuron* 24, 49–65.
- Singer, W., Gray, C.M., 1995. Visual feature integration and the temporal correlation hypothesis. *Annual review of neuroscience* 18, 555–586.
- Slovik, M., Rosin, B., Moshel, S., Mitelman, R., Schechtman, E., Eitan, R., Raz, A., Bergman, H., 2017. Ketamine induced converged synchronous gamma oscillations in the cortico-basal ganglia network of nonhuman primates. *Journal of neurophysiology* 118, 917–931.
- Softky, W.R., Koch, C., 1993. The highly irregular firing of cortical cells is inconsistent with temporal integration of random epsps. *Journal of neuroscience* 13, 334–350.
- Spencer, K.M., 2009. The functional consequences of cortical circuit abnormalities on gamma oscillations in schizophrenia: insights from computational modeling. *Frontiers in human neuroscience* 3, 33.
- Spencer, K.M., Nestor, P.G., Perlmutter, R., Niznikiewicz, M.A., Klump, M.C., Frumin, M., Shenton, M.E., McCarley, R.W., 2004. Neural synchrony indexes disordered perception and cognition in schizophrenia. *Proceedings of the National Academy of Sciences* 101, 17288–17293.
- Spencer, K.M., Niznikiewicz, M.A., Nestor, P.G., Shenton, M.E., McCarley, R.W., 2009. Left auditory cortex gamma synchronization and auditory hallucination symptoms in schizophrenia. *BMC neuroscience* 10, 1–13.
- Spencer, K.M., Salisbury, D.F., Shenton, M.E., McCarley, R.W., 2008.  $\gamma$ -band auditory steady-state responses are impaired in first episode psychosis. *Biological psychiatry* 64, 369–375.
- Stimberg, M., Brette, R., Goodman, D.F., 2019. Brian 2, an intuitive and efficient neural simulator. *eLife* 8, e47314. doi:10.7554/eLife.47314.
- Su, T., Lu, Y., Geng, Y., Lu, W., Chen, Y., 2018. How could n-methyl-d-aspartate receptor antagonists lead to excitation instead of inhibition? *Brain Science Advances* 4, 73–98.
- Susin, E., Destexhe, A., 2021. Integration, coincidence detection and resonance in networks of spiking neurons expressing gamma oscillations and asynchronous states. *PLOS Computational Biology* 17, e1009416.
- Suzuki, Y., Jodo, E., Takeuchi, S., Niwa, S., Kayama, Y., 2002. Acute administration of phencyclidine induces tonic activation of medial prefrontal cortex neurons in freely

- moving rats. *Neuroscience* 114, 769–779.
- Telenczuk, B., Telenczuk, M., Destexhe, A., 2020. A kernel-based method to calculate local field potentials from networks of spiking neurons. *Journal of Neuroscience Methods* 344, 108871.
- Tiesinga, P., Sejnowski, T.J., 2009. Cortical enlightenment: are attentional gamma oscillations driven by ping or pong? *Neuron* 63, 727–732.
- Uhlhaas, P.J., Singer, W., 2010. Abnormal neural oscillations and synchrony in schizophrenia. *Nature reviews neuroscience* 11, 100–113.
- Vinck, M., Womelsdorf, T., Buffalo, E.A., Desimone, R., Fries, P., 2013. Attentional modulation of cell-class-specific gamma-band synchronization in awake monkey area v4. *Neuron* 80, 1077–1089.
- Volk, D.W., Austin, M.C., Pierri, J.N., Sampson, A.R., Lewis, D.A., 2000. Decreased glutamic acid decarboxylase67 messenger rna expression in a subset of prefrontal cortical  $\gamma$ -aminobutyric acid neurons in subjects with schizophrenia. *Archives of general psychiatry* 57, 237–245.
- Vollenweider, F., Leenders, K., Øye, I., Hell, D., Angst, J., 1997. Differential psychopathology and patterns of cerebral glucose utilisation produced by (s)- and (r)-ketamine in healthy volunteers using positron emission tomography (pet). *European Neuropsychopharmacology* 7, 25–38.
- Wang, H.X., Gao, W.J., 2009. Cell type-specific development of nmda receptors in the interneurons of rat prefrontal cortex. *Neuropsychopharmacology* 34, 2028–2040.
- Widman, A.J., McMahon, L.L., 2018. Disinhibition of cal pyramidal cells by low-dose ketamine and other antagonists with rapid antidepressant efficacy. *Proceedings of the National Academy of Sciences* 115, E3007–E3016.
- Womelsdorf, T., Fries, P., Mitra, P.P., Desimone, R., 2006. Gamma-band synchronization in visual cortex predicts speed of change detection. *Nature* 439, 733–736.
- Wood, J., Kim, Y., Moghaddam, B., 2012. Disruption of prefrontal cortex large scale neuronal activity by different classes of psychotomimetic drugs. *Journal of Neuroscience* 32, 3022–3031.
- Zerlaut, Y., Destexhe, A., 2017. Enhanced responsiveness and low-level awareness in stochastic network states. *Neuron* 94, 1002–1009.
- Zhang, Y., Behrens, M.M., Lisman, J.E., 2008. Prolonged exposure to nmdar antagonist suppresses inhibitory synaptic transmission in prefrontal cortex. *Journal of neurophysiology* 100, 959–965.